DOI: 10.1002/cmdc.200900523

Design, Synthesis, and Preliminary Biological Evaluation of Pyrrolo[3,4-*c*]quinolin-1-one and Oxoisoindoline Derivatives as Aggrecanase Inhibitors

Andrea Cappelli,*[a] Chiara Nannicini,[a] Salvatore Valenti,[a] Germano Giuliani,[a] Maurizio Anzini,[a] Laura Mennuni,[b] Antonio Giordani,[b] Gianfranco Caselli,[b] Luigi Piero Stasi,[b] Francesco Makovec,[b] Gianluca Giorgi,[c] and Salvatore Vomero[a]

A small set of aggrecanase inhibitors based on the pyrrolo[3,4-*c*]-quinolin-1-one or oxoisoindoline frameworks bearing a 4-(benzyloxy)phenyl substituent and different zinc binding groups were rationally designed and evaluated in silico by docking studies using the crystal structure of the ADAMTS-5 catalytic domain (PDB code: 3B8Z). The designed compounds were synthesized via straightforward routes and tested for their potential inhibitory activity against ADAMTS-5 and ADAMTS-4. Among the compounds containing the pyrrolo[3,4-*c*]quinolinone tricyclic system, hydroxamate derivative **2b** inhibited both ADAMTS-5 and ADAMTS-4, with IC_{50} values in the submicromolar range and an inhibitory profile very similar to that of reference carboxylate derivative **11**. Conversely, the corresponding carboxylate derivative **2a** was significantly less active and unable to discriminate between ADAMTS-5 and -4. The structure–activity relationship analysis of pyrroloquinolinone derivatives **2a–i** suggests that the carboxylate or hydroxamate groups of compounds **2a**,**b** play a key role in the interaction of these compounds with ADAMTS-5 and -4. On the other hand, the oxoisoindoline derivatives **3a**,**b** lack significant ADAMTS-4 inhibitory activity and inhibit ADAMTS-5 showing IC_{25} values in the micromolar range.

Introduction

Osteoarthritis is a debilitating disease caused by degradation of aggrecan and collagen in the articular cartilage matrix leading to progressive and chronic inflammation, pain, and reduced mobility in the affected joint.[1] While collagen is the structural component of cartilage and provides strength to the tissue, aggrecan is the major cartilage proteoglycan, which forms a complex network of aggregates with hyaluronic acid and collagen to provide flexibility, elasticity, and resistance to compression in the articular cartilage.[2] Under physiologic conditions, the cartilage matrix is constantly remodeled through degradation followed by synthesis of type II collagen and aggrecan to maintain the integrity of the cartilage.[3] The loss of glycosaminoglycan-rich aggrecan fragments via proteolysis is the primary event leading to the destruction of the cartilage and is attributable to the activity of aggrecanase.[4] Current osteoarthritis treatments (e.g., corticosteroids, glucosamine, nonsteroidal anti-inflammatory drugs, intra-articular injections of hyaluronic acid conjugates) provide only symptomatic relief with no pharmacological therapy available to stop and/or reverse the progression of this disease.[5] In the end, the articular cartilage is eroded and joint replacement by surgery is required.

Aggrecanases are members of the "a disintegrin and metalloprotease with thrombospondin motifs" (ADAMTS) family of zinc metalloproteases. Both ADAMTS-4 (aggrecanase-1) and ADAMTS-5, (aggrecanase-2) have been shown to cleave aggrecan at the Glu 373—Ala 374 peptide bond in the interglobular domain (IGD).[6] Experiments with genetically modified mice, in which the catalytic domain of ADAMTS-5 was deleted, indicated that aggrecanase is the primary enzyme responsible for in vivo aggrecan degradation in both mechanical and inflammatory osteoarthritis murine models.[7]

Comparison of the features of ADAMTS-4 and ADAMTS-5 showed that, in terms of gene regulation, they are antithetical to each other. In fact, in most cases ADAMTS-5 is constitutively expressed in human condrocytes and synovial fibroblasts, whereas ADAMTS-4 expression is induced by proinflammatory cytokines.[8] Thus, selective aggrecanase inhibitors have become attractive for rational drug design, and a number of hydroxamate inhibitors were reported in very recent years.[9] However, the hydroxamate group is known to be a strong zinc-chelating moiety, which generally confers poor pharmacokinetic properties and low selectivity in the interaction with metalloproteases.[10] Structural modifications by the introduc-

[a] *Prof. A. Cappelli, Dr. C. Nannicini, Dr. S. Valenti, Dr. G. Giuliani, Prof. M. Anzini, Prof. S. Vomero*
Dipartimento Farmaco Chimico Tecnologico and the European Research Centre for Drug Discovery and Development, Università di Siena
Via A. Moro, 53100 Siena (Italy)
Fax: (+39) 057-723-4333
E-mail: cappelli@unisi.it

[b] *Dr. L. Mennuni, Dr. A. Giordani, Dr. G. Caselli, Dr. L. P. Stasi, Dr. F. Makovec*
Rottapharm S.p.A.
Via Valosa di Sopra 7, 20052 Monza (Italy)

[c] *Prof. G. Giorgi*
Dipartimento di Chimica, Università di Siena
Via A. Moro, 53100 Siena (Italy)

tion of polar groups in the region of the hydroxamate moiety were reported to show favorable effects (via an intramolecular hydrogen bond and steric hindrance) on absorption and clearance.[9a] Moreover, different zinc-binding groups (ZBGs) other than the hydroxamate moiety have been investigated to obtain matrix metalloproteinase inhibitors with improved absorption and clearance. For instance, a carboxylate moiety has become a common replacement for a hydroxamate group in the design of aggrecanase inhibitors, as well as other matrix metalloproteinase modulators.[11]

This paper describes the results of the initial investigation on ADAMTS inhibitors **2** and **3**. In this structure–activity relationship study, the effect of hydroxamate masking and replacement was evaluated in compounds based on planar pyrrolo[3,4-*c*]quinolin-1-one or oxoisoindoline frameworks.

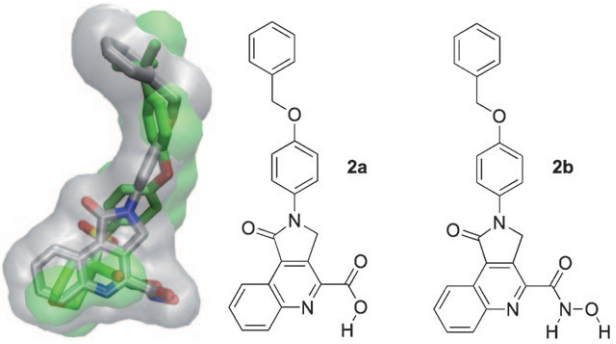

Figure 1. Superimposition of reference hydroxamate **1** (green) in its ADAMTS-5-bound conformation with compound **2b** (grey, van der Waals surfaces are given in order to show the funnel shape of the molecule). The structures of pyrrolo[3,4-*c*]quinolin-1-one derivatives **2a**,**b** are included for clarity.

Results and Discussion

Design of ADAMTS inhibitors

The recently published high-resolution crystal structure[12] of the ADAMTS-5 catalytic domain in the presence of a hydroxamate inhibitor **1** (PDB code: 3B8Z) shows a funnel shape for

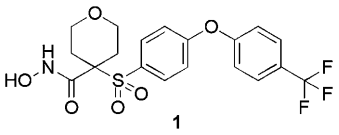

1

the catalytic site, which is open at the zinc site and terminates with a L-shaped hydrophobic channel at the opposite end.[12a] The enzyme–inhibitor complex exhibits a three-point interaction in which the hydroxamate group plays a key role by chelating the zinc atom and interacting with Glu 411. Furthermore, an additional hydrogen-bonding interaction and a specific strong hydrophobic interaction (within the S1′ pocket) are also established.

Our initial target was the design of aggrecanase inhibitors showing structurally simple, fairly rigid, and easily accessible scaffolds bearing substituents capable of establishing suitable interactions with the ADAMTS catalytic domain.

On the basis of its shape and dimension, a planar pyrrolo[3,4-*c*]quinolinone tricyclic system bearing the 4-(benzyloxy)-phenyl substituent of compounds **2** (Figure 1) was considered to represent an appropriate scaffold for the funnel-shaped ADAMTS-5 catalytic site that could be "decorated" with suitable ZBGs (e.g., COOH as in compound **2a**, or CONHOH as in compound **2b**).

In our design hypothesis, the quinoline nitrogen of compounds **2** was considered to be capable of masking (i.e., during the drug transport across membranes) polar ZBGs by forming an intramolecular hydrogen bond. On the other hand, compounds **3a**,**b** represent simplified analogues of pyrroloquinolinone derivatives **2a**,**b** in which the carbonyl oxygen atom should assist the ZBG in the chelating effect and mask polar ZBGs such as carboxylate and hydroxamate through the formation of an intramolecular hydrogen bond.

In order to evaluate the fitting of compounds **2a**,**b** and **3a**,**b** within the ADAMTS-5 catalytic domain, docking simulations were performed by means of AutoDock 4.0 (for details see the Experimental Section). Quinolinone derivatives **2a**,**b** appear to be capable of fitting the catalytic site of the ADAMTS-5 with good effectiveness (Figure 2) and similar short-range contacts, but with a subtle difference in the polar interactions. In particular, docking results suggest that hydroxamate derivative **2b** could establish an additional polar interaction (e.g., with Glu 411) compared with carboxylate derivative **2a**, which leads to the prediction of a higher potency for compound **2b**. The docking result obtained with quinoline derivative **2a** suggested the replacement of its polar carboxylate substituent with the different groups of compounds **2c**–**i** in order to obtain direct information about the polar interaction of compounds **2** with ADAMTS enzymes.

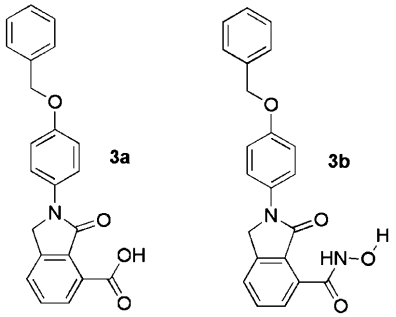

Similarly, the in silico predicted interaction of oxoisoindoline derivative **3a** with ADAMTS-5 catalytic site appears to be as effective as that predicted for **2a**. In fact, in the docked conformations (Figure 3), compound **3a** seems to be capable of coordinating the zinc ion by means of a bidentate interaction through the lactam carbonyl oxygen and the hydroxy group of the carboxylic moiety. Moreover, the docking results suggest

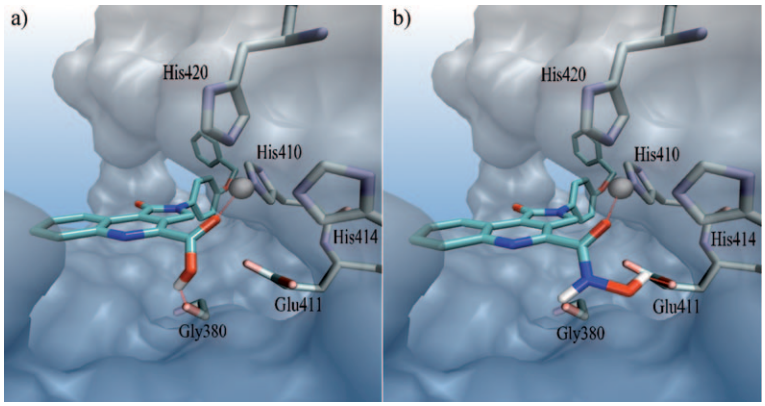

Figure 2. Pyrroloquinolinone derivatives a) **2a** and b) **2b** docked into the ADAMTS-5 catalytic site. The zinc ion is shown as a grey sphere. Coordinating and hydrogen bonds are represented as red dotted lines.

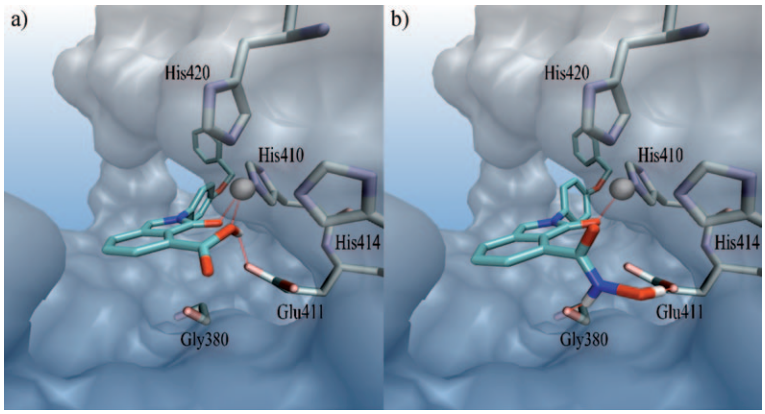

Figure 3. Oxoisoindoline derivatives a) **3a** and b) **3b** docked into the ADAMTS-5 catalytic site. The zinc ion is shown as a grey sphere. Coordinating and hydrogen bonds are represented as red dotted lines.

that the hydroxy group is involved in a hydrogen bond with Glu411. Similarly to pyrroloquinolinone derivatives **2a**,**b**, hydroxamate derivative **3b** is predicted to be capable of establishing a stronger interaction than the carboxylate derivative **3a**. However, it should be noted that in the docked conformations of **2a**,**b**, and **3a**,**b**, no intramolecular hydrogen bond is present. Therefore, our masking hypothesis could represent a critical point in the design of these compounds, because a too strong intramolecular hydrogen bond could prevent a favorable enzyme–inhibitor interaction.

Chemistry

Target pyrrolo[3,4-*c*]quinolin-1-one derivatives **2a–f** were synthesized by means of a multistep procedure described in Scheme 1–3. Pyrrolo[3,4-*c*]quinolin-1-one derivatives **2** were synthesized using chemistry previously developed for the synthesis of 5-HT_3 receptor ligands.[13] Compound **4**[13] was brominated and cyclized with 4-benzyloxyaniline (Scheme 1) to give the intermediate **2h**, which was hydrogenated in the presence of palladium on carbon to obtain the unsubstituted pyrroloquinolinone derivative **2g**. Suzuki cross-coupling of 2-chloroquinoline derivative **2h** with *N*-phenyldietanolamine 2-pyridilboronate[14] gave compound **2d**.

Imidoylchloride **2h** (Scheme 2) was subjected to Stille-type coupling reaction[15] with trimethylaluminum to give compound **2i**, which provided oxime **2c** via oxidation with SeO_2 to aldehyde **2e** and subsequent reaction with hydroxylamine hydrochloride. Alternatively, oxidation of aldehyde **2e** with hydrogen peroxide gave carboxylic acid **2a**. The conversion of **2a** into the corresponding hydroxamate **2b** was accomplished by coupling with *O*-(*tert*-butyldimethylsilyl)hydroxylamine in the presence of Castro's reagent (BOP)[16] and spontaneous deprotection.

Finally, compound **2i** was treated with *meta*-chloroperoxybenzoic acid (*m*-CPBA) to obtain quinoline *N*-oxide **6** in high yield (Scheme 3). Reaction of **6** with *p*-toluenesulfonyl chloride (TsCl) gave tosylate **7**, which provided methyl ether **2f** by reaction with magnesium turnings in methanol.[17]

Isoindoline derivatives **3a**,**b** were prepared from commercially available 3-methylphtalic anhydride **8** as shown in Scheme 4. Anhydride **8** was brominated with *N*-bromosuccinimide (NBS) in the presence of dibenzoyl peroxide following the literature[18] and cyclized with 4-benzyloxyaniline to give the expected carboxylic acid **3a**. The structure of carboxylic acid **3a** was confirmed by crystallographic studies, which showed the existence of an unexpectedly strong intramolecular hydrogen-bonding interaction between

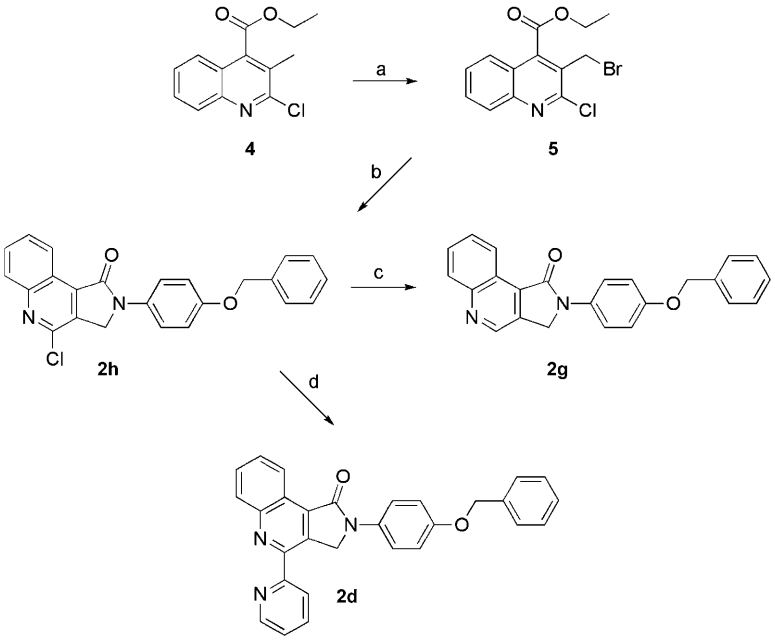

Scheme 1. Preparation of compounds **2d**, **g**, **h**. *Reagents and conditions*: a) NBS, benzoyl peroxide, CCl_4, reflux, 2.5 h, 79%; b) 4-benzyloxyaniline hydrochloride, K_2CO_3, EtOH, reflux, 1 h, 62%; c) H_2, Pd/C, $CHCl_3$, EtOH, Et_3N, RT, 30 h, 16%; d) PPh_3, $Pd(OAc)_2$, K_2CO_3, CuI, *N*-phenyldietanolamine 2-pyridilboronate, THF, reflux, 10 min, 9%.

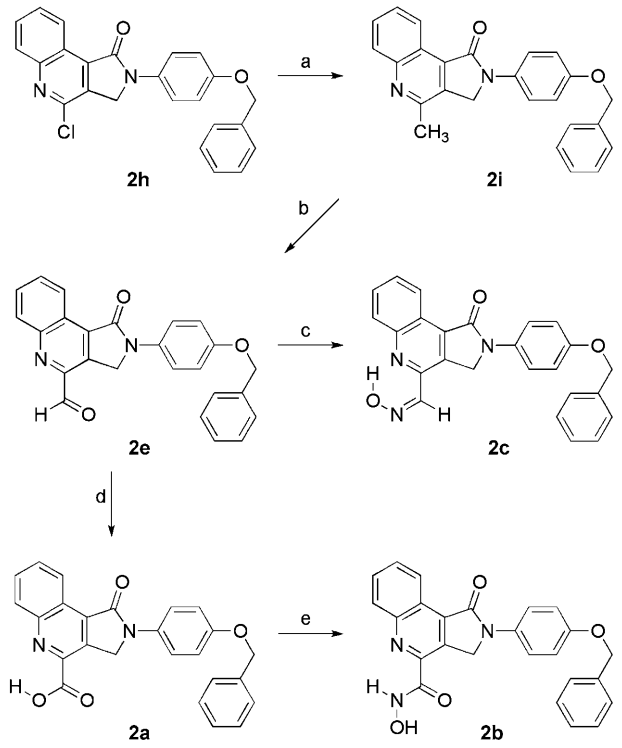

Scheme 2. Preparation of compounds **2a**–**c**,**e**,**i**. *Reagents and conditions*: a) $Al(CH_3)_3$, $Pd(PPh_3)_2Cl_2$, LiCl, DMF, 85 °C, 2 h, 47%; b) SeO_2, dioxane, reflux, 45 min, 71%; c) $NH_2OH{\cdot}HCl$, pyridine, RT, 30 min, 78%; d) H_2O_2, H_2O, HCOOH, RT, overnight, 96%; e) *O*-(*tert*-butyldimethylsilyl)hydroxylamine, BOP, Et_3N, DMF, RT, overnight, 48%.

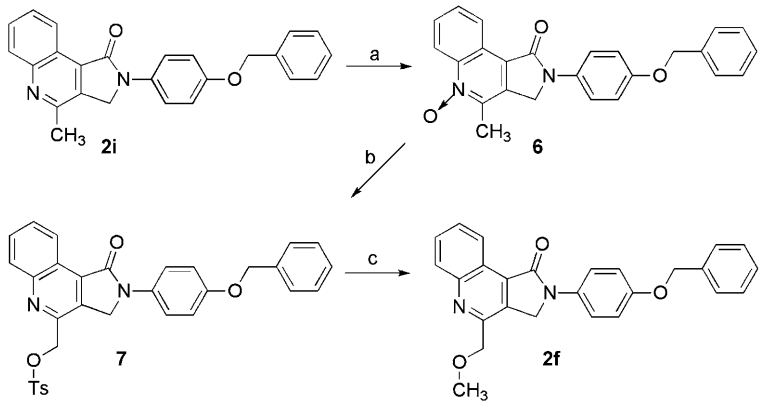

Scheme 3. Preparation of compound **2f**. *Reagents and conditions*: a) *m*-CPBA, CH_2Cl_2, RT, overnight, 52%; b) TsCl, K_2CO_3, $CHCl_3$, H_2O, reflux, overnight, 54%; c) Mg, MeOH, reflux, 2 h, 18%.

the acid proton and lactam carbonyl oxygen atom (Figure 4).

The ^{1}H NMR spectrum of compound **3a**, performed in both deuterated chloroform and deuterated dimethyl sulfoxide, showed the peak attributable to acid proton to resonate at 15.5–15.7 ppm, indicating that the hydrogen-bonding interaction is rather strong in the organic solvents used. This result supports the postulated masking effect in the hydrophobic environment, but it raises questions about the hydrogen bond stability in the aggrecanase active site that leads to the formation of a pseudocycle and could prevent a favorable interaction with the zinc atom (see Figure 3). Similarly to **3a**, crystallographic studies of **3b** showed that its NH proton interacts with the lactam carbonyl oxygen atom in the solid-state structure (Figure 5).

Also, in compound **10** (Figure 6), the carboxylic proton appears to interact strongly with the imidate nitrogen atom, and the ^{1}H NMR spectra of **10** show a very low-field resonance at 18.8 ppm in both deuterated chloroform and deuterated dimethyl sulfoxide.

Therefore, the X-ray crystal structures of compounds **3a**,**b** and **10** show, as a common feature, the occurrence of strong intramolecular hydrogen-bonding interactions involving the COOH and the lactam carbonyl oxygen atom (**3a**), the hydroxamic NH group and the lactam carbonyl oxygen atom (**3b**), the COOH and the imidate nitrogen atom in **10** (Table 1 and Table 2). In all the three compounds, the existence of these interactions causes the formation of a seven-membered ring in which one bond is due to the proton···acceptor interaction that, in the three compounds, averages 1.68 Å (in the range of the partially covalent hydrogen bonds[19]). The presence of a rigid bicyclic planar system does not facilitate the formation of a reasonable proton···acceptor distance; this hydrogen bond can only be obtained by distortion of the bond angles involving the acidic moiety. Indeed, significant distortions of the C(4)–C(5)–C(10) and C(6)–C(5)–C(10) bond angles from the theoretical value of 120° are observed. In particular, the former is wider (mean = 128.1°) so as to allow a longer distance proton···acceptor interaction, while, as a consequence, the latter is narrower (mean = 115.4°) than the theoretical value (120°). Moreover, compound **10** also shows two strong intermolecular hydrogen-bonding interactions: O(4)–H(*x*,*y*,*z*)···O2(-*x*,1-*y*,2-*z*) and O(2)(*x*,*y*,*z*)···H-O(4)(-*x*,1-*y*,2-*z*) with H···O distance equal to 1.82 Å

Table 1. Intramolecular hydrogen-bonding interactions and significant geometrical features in the X-ray crystal structures of compounds **3a**,**b** and **10**.

Compd	Donor (D)	Acceptor (A)	D–H [Å][a]	H···A [Å][a]	D···A [Å][a]	D–H···A [°][a]
3a	O(3A)–H	O(1A)	0.82	1.74	2.541(6)	164
	O(3B)–H	O(1B)	0.82	1.71	2.524(6)	177
3b	N(3)–H	O(1)	1.10(5)	1.56(6)	2.618(5)	159(5)
10	O(4)–H	N(1)	0.82	1.72	2.521(5)	164

[a] Numbers in parentheses are the standard deviations.

In vitro ADAMTS inhibitory activity

Potential aggrecanases inhibitors **2a–i** and **3a**,**b** were screened for protease action at the "signature" cleavage site Glu373–Ala374 in the IGD. In fact, this cleavage releases the entire glycosaminoglican-containing portion of aggrecan and may have

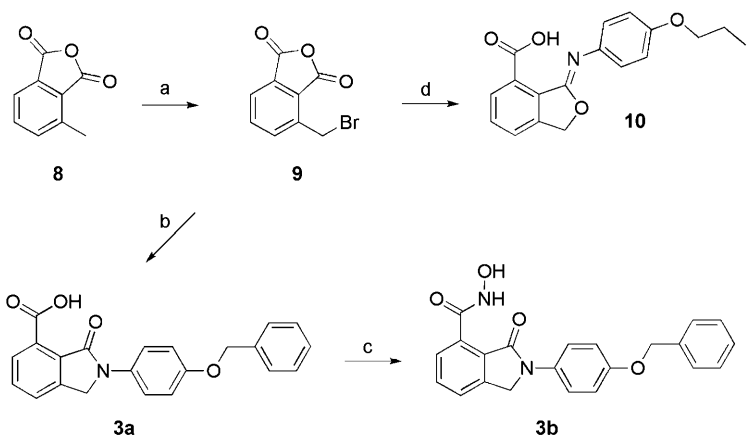

Scheme 4. Preparation of compound **3a**,**b** and **10**. *Reagents and conditions*: a) NBS, benzoyl peroxide, CCl_4, reflux, 4 h, 66%; b) 4-benzyloxyaniline hydrochloride, K_2CO_3, EtOH, reflux, 45 min, 29%; c) *O*-(*tert*-butyldimethylsilyl)hydroxylamine, BOP, Et_3N, DMF, RT, overnight, 51%; d) $NH_2C_6H_4OCH_2CH_2CH_3$, K_2CO_3, EtOH, reflux, 45 min, 14%.

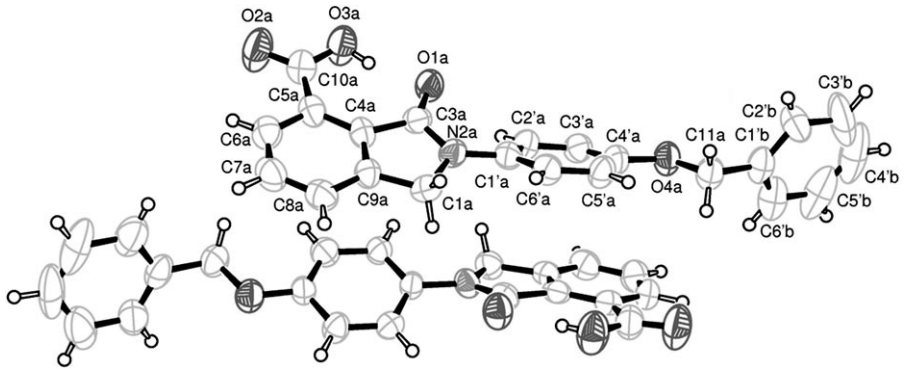

Figure 4. Two molecules form the asymmetric unit of **3a**. Ellipsoids enclose 50% probability.

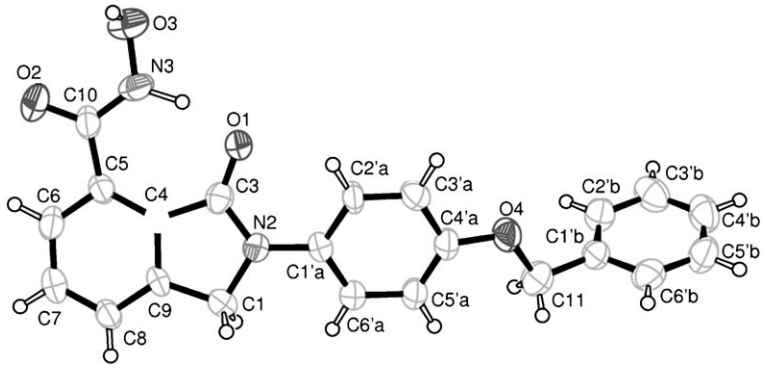

Figure 5. Crystal structure of compound **3b**. Ellipsoids enclose 50% probability.

Table 2. Significant bond angles in the X-ray crystal structures of compounds **3a**,**b**, and **10**.[a]

Compd	C(4)–C(5)–C(10)	C(6)–C(5)–C(10)	C(4)–C(5)–C(6)
3a	128.4(6)	115.7(6)	115.9(6)
	128.3(6)	115.2(6)	116.5(6)
3b	128.8(4)	113.8(4)	117.3(4)
10	127.2(5)	117.1(4)	115.7(4)

[a] Numbers in parentheses are the standard deviations.

the most deleterious effects on the loss of the mechanical properties of cartilage.[20] Moreover, in vivo studies showed that blocking aggrecanolysis in the aggrecan IGD alone protects against cartilage erosion and may promote cartilage repair.[6a] Thus, compounds **2a**–**i** and **3a**,**b** were tested for their potential inhibitory activity against ADAMTS-4 and ADAMTS-5 enzymes by means of the InviLISA aggrecanase assay (Invitek GmbH, Berlin) in comparison with reference compounds **11**[21] and **12**.[9d] A recombinant fragment of human aggrecan IGD (aggrecan–IGD; Thr331–Gly458) was used as a substrate, and the assay was carried out in two steps according to Will and coworkers[22] (for details see the Experimental Section).

The results, summarized in Table 3, show that carboxylate derivative **2a** appears to be capable of inhibiting both ADAMTS-5 and ADAMTS-4, showing IC_{50} values (half maximal inhibitory concentration) in the micromolar range, and is about one order of magnitude less potent than the reference carboxylate derivative **11** at inhibiting ADAMTS-5. On the other hand, the corresponding hydroxamic acid **2b** is significantly more potent than carboxylic acid **2a** and appears to discriminate appreciably between ADAMTS-5 and -4. However, the inhibitory potencies shown by **2b** are different from those obtained with reference hydroxamate **12**. The remaining quinolinone derivatives **2c**–**i** (bearing less polar substituents) show inhibition values below 40% at the maximum concentration tested (10 μM). Thus, the results obtained with pyrroloquinolinone derivatives **2a**–**i** confirmed the key role of the carboxylate group, or hydroxamate group of compounds **2a**,**b**, in the interaction with ADAMTS-5 and -4.

The results obtained with oxoisoindoline derivatives **3a**,**b** show that these compounds lack significant ADAMTS-4 inhibitory activity and show a particular behavior in inhibiting ADAMTS-5. In fact, the inhibition curves of compounds **3a**,**b** show an apparent plateau at ~50% inhibition. The IC_{25} values calculated show that ADAMTS-5 inhibitory activity is in the micromolar range and slightly higher in the hydroxamate derivative **3b** with respect to the corresponding carboxylate **3a**, as anticipated by the docking studies. The behavior shown by **3a**,**b** in inhibiting ADAMTS-5 may be related to solubility problems, probably caused by the presence of planar moieties (prone to forming stacked aggregates as suggested by Figure 4) and the particularly strong intramolecular hydrogen bonds originally designed to mask polar ZBGs. Specifically, the dilution of the clear dimethyl sulfoxide stock solution to obtain the first working solution (DMSO concentration of ~10%)

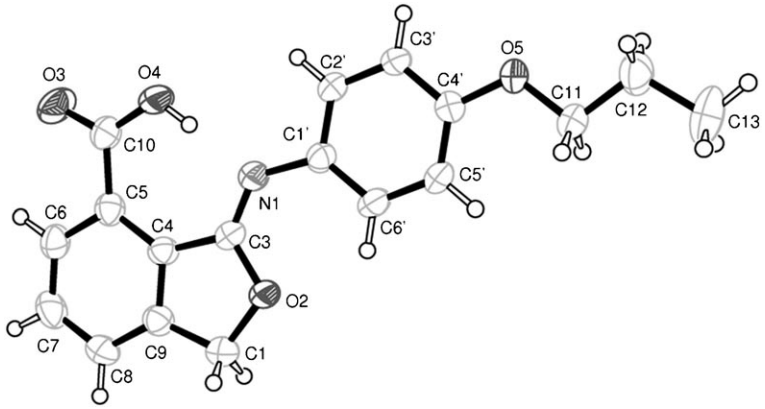

Figure 6. Crystal structure of compound **10**. Ellipsoids enclose 50% probability.

Table 3. In vitro inhibitory activity of compounds **2a–i**, **3a,b** and reference compounds **11** and **12** against ADAMTS-4 and ADAMTS-5.

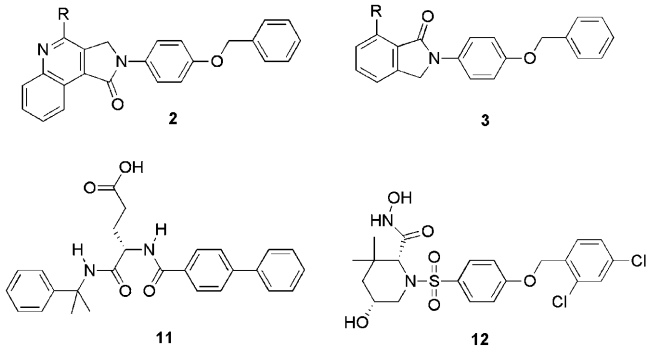

2 **3**

11 **12**

Compd	R	IC_{50} [μM] ADAMTS-4	ADAMTS-5
2a	COOH	15 ± 2.1	12 ± 1.8
2b	C(O)NHOH	0.21 ± 0.05	0.95 ± 0.11
2c	CH=NOH	NA[b]	34%[a]
2d	2-pyridyl	NA[b]	NA[b]
2e	CHO	NT[c]	NA[b]
2f	CH_2OCH_3	NA[b]	27%[a]
2g	H	NA[b]	NA[b]
2h	Cl	32%[a]	NA[b]
2i	CH_3	NA[b]	32%[a]
3a	COOH	NA[b]	7.5 ± 3.1[d]
3b	C(O)NHOH	NA[b]	2.5 ± 0.44[d]
11		0.21 ± 0.04	1.1 ± 0.21
12		0.0011 ± 0.00030	0.0014 ± 0.00020

[a] Values expressed as a percentage represent inhibition of enzyme activity at 10 μM. [b] NA: not active at 10 μM. [c] NT: not tested. [d] IC_{25} values (μM) given because compounds **3a,b** showed a plateau inhibition at ~50%.

caused opalescence, which suggests that a partial precipitation occurred. The incomplete solubility of **3a,b** in the conditions used in the enzymatic tests may lead to an underestimation of the ADAMTS activity of these compounds.

Conclusions

A small series of aggrecanase inhibitors based on the planar pyrrolo[3,4-*c*]quinolin-1-one (compounds **2**) or oxoisoindoline (compounds **3**) frameworks bearing a 4-(benzyloxy)-phenyl substituent and different ZBGs have been designed and evaluated in silico by docking studies using the crystal structure of the ADAMTS-5 catalytic domain (PDB code: 3B8Z). Molecular modeling predicts the good fit of compounds **2a,b** and **3a,b** within the enzyme cleft, with hydroxamate derivatives **2b** and **3b** predicted to show slightly superior binding features with respect to the corresponding carboxylate derivatives **2a** and **3a**.

Compounds **2a–i** and **3a,b** were synthesized via straightforward procedures, and crystallographic studies revealed that the polar (carboxylic or hydroxamic) groups of compounds **3a,b** are involved in unexpectedly strong intramolecular hydrogen bonds. The newly synthesized compounds were evaluated for their potential to inhibit ADAMTS-4 and ADAMTS-5 (InviLISA aggrecanase assay). Among the compounds containing the pyrrolo[3,4-*c*]quinolinone tricyclic system, hydroxamate derivative **2b** appears to be capable of inhibiting both ADAMTS-5 and ADAMTS-4, with IC_{50} values in the submicromolar range. It is worth remarking that the inhibitory profile shown by **2b** is very similar to that found for reference carboxylate derivative **11**. Conversely, the corresponding carboxylate derivative **2a** is significantly less active and unable to discriminate between ADAMTS-5 and 4. The structure–activity relationships within the pyrroloquinolinone derivatives (**2a–i**) prove the key role played by the contacts established between the polar groups of compounds **2a,b** and the ADAMTS-4 and -5 enzymes. The simplified analogues **3a,b** show different enzyme interactions compared with the corresponding pyrroloquinolinone derivatives **2a,b**. In fact, compounds **3a,b** lack significant ADAMTS-4 inhibitory activity but inhibit ADAMTS-5 in the micromolar range.

In summary, this study represents a successful approach to the design of ADAMTS inhibitors possessing simple structures and syntheses (especially in the case of oxoisoindoline derivatives **3a,b**) for which unanticipated solubility features have prevented further development.

Experimental Section

Chemistry

All chemicals used were reagent grade. Yields refer to purified products and are not optimized. Melting points were determined in open capillaries on a Gallenkamp apparatus and are uncorrected. Merck silica gel 60 (230–400 mesh) was used for column chromatography. Merck TLC plates, silica gel 60 F_{254} were used for TLC. ^{1}H NMR spectra were recorded at 200 MHz (Bruker AC200 spectrometer) or at 400 MHz (Bruker DRX-400 AVANCE spectrometer) in the indicated solvents (TMS as internal standard). Chemical shifts (δ) are expressed in parts per million (ppm), and the coupling constants (J) are given in Hz. An Agilent 1100 LC/MSD operating with a electrospray source was used in mass spectrometry experiments; unless otherwise stated, experiments were carried out in the positive mode. Microanalyses were carried out using a Perkin–Elmer Series II CHNS/O Analyzer 2400.

2-[4-(Benzyloxy)phenyl]-4-chloro-2,3-dihydro-1*H*-pyrrolo[3,4-*c*]-quinolin-1-one (2h): A mixture of **5**[13] (1.31 g, 4.0 mmol), 4-(benzyloxy)aniline hydrochloride (1.04 g, 4.4 mmol) and K_2CO_3 (0.61 g, 4.4 mmol) in EtOH (20 mL) was refluxed for 1 h. The reaction mixture was allowed to cool to RT and the precipitate was collected by filtration, and washed in sequence with H_2O and EtOH/EtOAc to give compound **2h** as a pale yellow solid (1.0 g, 62%); mp: 214–215 °C; ^{1}H NMR (200 MHz, $CDCl_3$): 4.91 (s, 2H), 5.11 (s, 2H), 7.07 (d, J=8.8, 2H), 7.33–7.43 (m, 5H), 7.70–7.87 (m, 4H), 8.14 (d, J=8.3, 1H), 9.11 ppm (d, J=7.7, 1H); ^{13}C NMR (100 MHz, $CDCl_3$): δ=49.8, 70.3, 115.6, 121.9, 122.9, 123.8, 127.5, 128.1, 128.7, 131.1, 131.8, 133.3, 136.8, 138.2, 144.8, 148.6, 156.5, 165.6 ppm; MS (ESI): *m/z* 423 $[M+Na]^+$; Anal. calcd for $C_{24}H_{17}ClN_2O_2\cdot\frac{3}{4}H_2O$: C 69.57, H 4.50, N 6.76, found: C 69.40, H 4.18, N 6.53.

2-[4-(Benzyloxy)phenyl]-2,3-dihydro-1*H*-pyrrolo[3,4-*c*]quinolin-1-one (2g): A mixture of **2h** (0.10 g, 0.25 mmol), Et_3N (0.1 mL) and 10% Pd/C (0.03 g) in $CHCl_3$/EtOH (30 mL; 1:1) was hydrogenated under atmospheric pressure at RT for 30 h. The catalyst was filtered off, and the filtrate was evaporated in vacuo. The residue was partitioned between $CHCl_3$ and H_2O. The organic layer was dried over Na_2SO_4 and concentrated in vacuo. Purification of the residue by flash chromatography (CH_2Cl_2/EtOAc; 8:2) gave **2g** as a pale yellow solid (0.015 g, 16%); mp: 194–196 °C; ^{1}H NMR (200 MHz, $CDCl_3$): δ=4.92 (s, 2H), 5.07 (s, 2H), 7.03 (d, J=8.9, 2H), 7.28–7.41 (m, 5H), 7.66–7.83 (m, 4H), 8.20 (d, J=8.2, 1H), 9.04–9.18 ppm (m, 2H); MS (ESI): *m/z* 389 $[M+Na]^+$; Anal. calcd for $C_{24}H_{18}N_2O_2\cdot\frac{1}{3}H_2O$: C 77.40, H 5.05, N 7.52, found: C 77.35, H 4.84, N 7.28.

2-[4-(Benzyloxy)phenyl]-2,3-dihydro-4-(pyridin-2-yl)-1*H*-pyrrolo-[3,4-*c*]quinolin-1-one (2d): A mixture of compound **2h** (0.20 g, 0.50 mmol), *N*-phenyldiethanolamine 2-pyridylboronate (0.27 g, 1.0 mmol), PPh_3 (0.030 g, 0.11 mmol), $Pd(OAc)_2$ (6.0 mg, 0.027 mmol), K_2CO_3 (0.14 g, 1.0 mmol) and CuI (0.040 g, 0.21 mmol) in THF (10 mL) was heated to reflux under N_2 for 10 min. The reaction mixture was then cooled to RT and the solvent removed in vacuo. The residue was partitioned between H_2O and $CHCl_3$ and the organic layer was dried over Na_2SO_4 and evaporated in vacuo. Purification of the residue by flash chromatography (CH_2Cl_2/EtOAc; 8:2) gave **2d** as a yellow solid (20 mg, 9%); mp: 205–206 °C; ^{1}H NMR (200 MHz, $CDCl_3$): δ=5.11 (s, 2H), 5.53 (s, 2H), 7.08 (m, 2H), 7.31–7.47 (m, 6H), 7.68–7.95 (m, 5H), 8.26 (d, J=8.4, 1H), 8.73–8.79 (m, 2H), 9.25 ppm (d, J=7.6, 1H); MS (ESI): *m/z* 444 $[M+H]^+$; Anal. calcd for $C_{29}H_{21}N_3O_2\cdot\frac{1}{3}H_2O$: C 77.49, H 4.86, N 9.35, found: C 77.29, H 4.56, N 9.22.

2-[4-(Benzyloxy)phenyl]-4-methyl-2,3-dihydro-1*H*-pyrrolo[3,4-*c*]-quinolin-1-one (2i): A solution of **2h** (1.0 g, 2.5 mmol) in dry DMF (10 mL) under Ar was treated with $Al(CH_3)_3$ (2.0 M in toluene; 1.2 mL, 2.4 mmol), LiCl (0.30 g, 7.1 mmol) and $Pd(PPh_3)_2Cl_2$ (0.080 g, 0.11 mmol). The resulting mixture was heated at 85 °C for 2 h, then poured into ice, neutralized with HCl (3 N), and extracted with CH_2Cl_2. The organic layer was dried over Na_2SO_4 and evaporated in vacuo. The residue was washed with EtOH to give **2i** as a light brown solid (0.45 g, 47%); mp: 183–185 °C; ^{1}H NMR (200 MHz, $CDCl_3$): δ=2.78 (s, 3H), 4.85 (s, 2H), 5.09 (s, 2H), 7.08 (m, 2H), 7.31–7.46 (m, 5H), 7.61–7.80 (m, 4H), 8.12 (d, J=8.3, 1H), 9.08 ppm (d, J=7.9, 1H); ^{13}C NMR (100 MHz, $CDCl_3$): δ=21.8, 49.8, 70.3, 115.4, 121.7, 122.4, 123.4, 127.5, 127.6, 128.0, 128.6, 128.8, 129.9, 132.3, 133.4, 134.8, 136.8, 148.2, 153.2, 156.2, 166.9 ppm; MS (ESI): *m/z* 381 $[M+H]^+$; Anal. calcd for $C_{25}H_{20}N_2O_2\cdot\frac{1}{4}H_2O$: C 78.00, H 5.37, N 7.28, found: C 78.04, H 5.18, N 7.14.

2-[4-(Benzyloxy)phenyl]-2,3-dihydro-1-oxo-1*H*-pyrrolo[3,4-*c*]quinoline-4-carbaldehyde (2e): A solution of **2i** (0.18 g, 0.47 mmol) in dioxane (10 mL) was treated with SeO_2 (0.30 g, 2.7 mmol) and refluxed for 45 min. The reaction was partitioned between CH_2Cl_2 and H_2O and separated. The organic layer was washed with H_2O, dried over Na_2SO_4, and evaporated in vacuo. Purification of the residue by flash chromatography (CH_2Cl_2/EtOAc; 95:5) gave **2e** as a thick yellow oil (0.132 g, 71%); ^{1}H NMR (200 MHz, $CDCl_3$): δ=5.09 (s, 2H), 5.25 (s, 2H), 7.06 (m, 2H), 7.31–7.42 (m, 5H), 7.79–7.94 (m, 4H), 8.36 (m, 1H), 9.22 (m, 1H), 10.34 ppm (s, 1H); MS (ESI): *m/z* 395 $[M+H]^+$.

(*Z*)-2-[4-(Benzyloxy)phenyl]-2,3-dihydro-1-oxo-1*H*-pyrrolo[3,4-*c*]-quinoline-4-carbaldehyde oxime (2c): A solution of **2e** (0.030 g, 0.076 mmol) in pyridine (2 mL) was treated with hydroxylamine hydrochloride (0.014 g, 0.20 mmol) and stirred for 30 min at RT. The solvent was removed in vacuo and the residue washed in sequence with H_2O and with CH_2Cl_2 to give compound **2c** as a yellow solid (24 mg, 78%); mp: 225–226 °C; ^{1}H NMR (200 MHz, [D$_6$]DMSO): δ=5.10 (s, 2H), 5.19 (s, 2H), 7.11 (d, J=8.8, 2H), 7.30–7.46 (m, 5H), 7.73–7.89 (m, 4H), 8.15 (d, J=8.1, 1H), 8.39 (s, 1H), 9.01 (d, J=8.2, 1H), 12.22 ppm (s, 1H): The chemical shift values of the signal attributed to aldoxime OH (12.22 ppm) and CH (8.39 ppm) groups were used in the configuration assignment according to Kleinspehn et al.[23]; ^{13}C NMR (100 MHz, [D$_6$]DMSO): δ= 52.4, 69.9, 115.7, 122.4, 122.7, 123.2, 128.2, 128.3, 128.9, 129.3, 129.7, 130.7, 132.6, 133.6, 135.3, 137.5, 147.5, 148.3, 150.4, 156.0, 166.0 ppm; MS (ESI): *m/z* 410 $[M+H]^+$; Anal. calcd for $C_{25}H_{19}N_3O_3\cdot\frac{2}{3}H_2O$: C 71.25, H 4.86, N 9.97, found: C 71.11, H 4.57, N 9.81.

2-[4-(Benzyloxy)phenyl]-2,3-dihydro-1-oxo-1*H*-pyrrolo[3,4-*c*]quinoline-4-carboxylic acid (2a): A solution of **2e** (0.13 g, 0.33 mmol) in formic acid (7.0 mL) was treated with H_2O_2 (4.0 mL, 3% *w/v* in H_2O). The reaction mixture was stirred overnight at RT and extracted with CH_2Cl_2. The organic layer was dried over Na_2SO_4 and evaporated in vacuo. Purification of the residue by washing with Et_2O gave **2a** as a red solid (0.13 g, 96%); mp: 197–199 °C; ^{1}H NMR (200 MHz, $CDCl_3$): δ=5.14 (s, 2H), 5.34 (s, 2H), 7.12 (d, J=9.0, 2H), 7.32–7.47 (m, 5H), 7.84 (d, J=9.0, 2H), 7.89–7.98 (m, 2H), 8.30 (d, J=8.2, 1H), 9.10 (d, J=8.0, 1H), 13.81 ppm (br s, 1H); ^{13}C NMR (100 MHz, [D$_6$]DMSO): δ=51.5, 69.4, 115.2, 122.0, 122.7, 123.9, 127.6, 127.8, 128.4, 130.2, 130.4, 130.6, 132.0, 135.6, 135.8, 137.0, 143.6, 146.7, 155.6, 165.3, 165.6 ppm; MS (ESI−): *m/z* 409 $[M-H]^-$; Anal. calcd for $C_{25}H_{18}N_2O_4\cdot\frac{1}{4}CHCl_3$: C 68.88, H 4.18, N 6.36, found: C 68.96, H 4.24, N 5.96.

2-[4-(Benzyloxy)phenyl]-2,3-dihydro-*N*-hydroxy-1-oxo-1*H*-pyrrolo[3,4-*c*]quinoline-4-carboxamide (2b): A solution of **2a** (0.060 g, 0.146 mmol) in dry DMF (10 mL) was treated with Castro's reagent (BOP; 0.065 g, 0.147 mmol), Et_3N (60 μL), and *O*-(*tert*-butyldimethylsilyl)hydroxylamine (0.035 g, 0.24 mmol) and stirred overnight at RT. The solvent was evaporated in vacuo, and the residue was purified by washing with H_2O, CH_2Cl_2, and Et_2O to give **2b** as a yellow solid (30 mg, 48%); mp: 163 °C (decomp); ^{1}H NMR (200 MHz, [D$_6$]DMSO): δ=5.13 (s, 2H), 5.36 (s, 2H), 7.12 (d, J=9.0, 2H), 7.34–7.43 (m, 5H), 7.80–7.94 (m, 4H), 8.22 (d, J=8.0, 1H), 9.08 (d, J=7.8, 1H), 9.30 (s, 1H), 11.73 ppm (s, 1H); MS (ESI−): *m/z* 424 $[M-H]^-$; Anal. calcd for $C_{25}H_{19}N_3O_4\cdot\frac{3}{4}CHCl_3$: C 60.06, H 3.87, N 8.16, found: C 59.89, H 4.08, N 7.88.

2-[4-(Benzyloxy)phenyl]-4-methyl-2,3-dihydro-1*H*-pyrrolo[3,4-*c*]-quinolin-1-one 5-oxide (6): A mixture of **2i** (0.60 g, 1.6 mmol) in 10 mL of CH_2Cl_2 with 0.66 g (3.8 mmol) of *m*-CPBA was stirred overnight at RT. After this time, the reaction mixture was washed in sequence with a 5% aq solution of K_2CO_3 and H_2O. The organic layer was dried over Na_2SO_4 and evaporated in vacuo. Purification of the

residue by flash chromatography (CH_2Cl_2/EtOAc; 1:1) gave **6** as a yellow solid (0.33 g, 52%); mp: 150–152 °C; ^{1}H NMR (200 MHz, $CDCl_3$): δ = 2.62 (s, 3H), 4.78 (s, 2H), 5.06 (s, 2H), 7.01 (d, J = 8.8, 2H), 7.27–7.40 (m, 5H), 7.62–7.78 (m, 4H), 8.68 (d, J = 8.7, 1H), 9.04 ppm (d, J = 8.2, 1H); ^{13}C NMR (100 MHz, $CDCl_3$): δ = 14.3, 49.5, 70.3, 115.5, 119.7, 121.6, 123.2, 124.2, 124.3, 127.5, 128.1, 128.6, 129.4, 130.5, 132.1, 135.3, 136.8, 140.7, 141.8, 156.2, 165.9 ppm; MS (ESI): m/z 419 $[M+Na]^+$.

[2-[4-(Benzyloxy)phenyl]-2,3-dihydro-1-oxo-1*H*-pyrrolo[3,4-*c*]quinolin-4-yl]methyl 4-methylbenzenesulfonate (7): A solution of TsCl (0.11 g, 0.58 mmol) and **6** (0.18 g, 0.45 mmol) in $CHCl_3$ (5.0 mL) was treated with a 10% aq solution of K_2CO_3 (5.0 mL). The resulting mixture was refluxed overnight with vigorous stirring. The reaction was partitioned between CH_2Cl_2 and H_2O, and the organic layer was washed with H_2O, dried over Na_2SO_4, and evaporated in vacuo. Purification of the residue by flash chromatography (petroleum ether/EtOAc; 3:7) gave **7** as a glassy solid (0.134 g, 54%); ^{1}H NMR (200 MHz, $CDCl_3$): δ = 2.39 (s, 3H), 5.01 (s, 2H), 5.11 (s, 2H), 5.47 (s, 2H), 7.07 (m, 2H), 7.24–7.47 (m, 7H), 7.68–7.89 (m, 6H), 8.08 (d, J = 8.8, 1H), 9.14 ppm (d, J = 8.0, 1H); MS (ESI): m/z 573 $[M+Na]^+$.

2-[4-(Benzyloxy)phenyl]-4-(methoxymethyl)-2,3-dihydro-1*H*-pyrrolo[3,4-*c*]quinolin-1-one (2f): A mixture of **7** (0.050 g, 0.091 mmol) in MeOH (8.0 mL) and Mg turnings (0.025 g, 0.10 mmol) was refluxed for 2 h. The cooled reaction mixture was neutralized with HCl (3 N) and partitioned between CH_2Cl_2 and H_2O. The organic layer was dried over Na_2SO_4 and evaporated in vacuo. Purification of the residue by flash chromatography (petroleum ether/EtOAc; 1:1) gave **2f** as a light brown solid (6.7 mg, 18%); mp: 195–197 °C; ^{1}H NMR (200 MHz, $CDCl_3$): δ = 3.50 (s, 3H), 4.92 (s, 2H), 5.04 (s, 2H), 5.09 (s, 2H), 7.06 (m, 2H), 7.29–7.42 (m, 5H), 7.61–7.80 (m, 4H), 8.15 (d, J = 7.8, 1H), 9.15 ppm (m, 1H); MS (ESI): m/z 411 $[M+H]^+$; Anal. calcd for $C_{26}H_{22}N_2O_3 \cdot \frac{2}{3}H_2O$: C 73.92, H 5.57, N 6.63, found: C 73.84, H 5.30, N 6.27.

2-[4-(Benzyloxy)phenyl]-3-oxoisoindoline-4-carboxylic acid (3a): A solution of **9** (0.20 g, 0.83 mmol) in EtOH (15 mL) was treated with K_2CO_3 (0.13 g, 0.94 mmol) and 4-(benzyloxy)aniline hydrochloride (0.22 g, 0.93 mmol) and refluxed for 45 min. The solvent was removed in vacuo and the residue partitioned between H_2O and EtOAc. The organic layer was dried over Na_2SO_4 and evaporated in vacuo. Purification of the residue by washing with EtOH and subsequent recrystallization (acetone/EtOH) gave **3a** as colorless crystals suitable for crystallographic studies (87 mg, 29%); mp: 180–181 °C; ^{1}H NMR (200 MHz, $CDCl_3$): δ = 4.96 (s, 2H), 5.09 (s, 2H), 7.05 (d, J = 8.5, 2H), 7.35–7.41 (m, 5H), 7.60–7.79 (m, 4H), 8.43 (m, 1H), 15.60 ppm (br s, 1H); MS (ESI): m/z 382 $[M+Na]^+$.

2-[4-(Benzyloxy)phenyl]-*N*-hydroxy-3-oxoisoindoline-4-carboxamide (3b): A solution of **3a** (0.030 g, 0.083 mmol) in dry DMF (5.0 mL) was treated with BOP (0.040 g, 0.090 mmol), Et_3N (28 μL), and O-(*tert*-butyldimethylsilyl)hydroxylamine (0.015 g, 0.10 mmol) and stirred overnight at RT. The solvent was evaporated in vacuo, and the residue was purified by washing with CH_2Cl_2 and subsequent recrystallization ($CHCl_3$/MeOH) by slow evaporation of the solvents to give **3b** as pale yellow crystals (16 mg, 51%); mp: 193–194 °C; ^{1}H NMR (200 MHz, [D_6]DMSO): δ = 5.03 (s, 2H), 5.13 (s, 2H), 7.09 (m, 2H), 7.34–7.42 (m, 5H), 7.70–7.78 (m, 4H), 8.07 (m, 1H), 9.24 (s, 1H), 12.95 ppm (s, 1H); MS (ESI): m/z 397 $[M+Na]^+$.

(*Z*)-3-(4-Propoxyphenylimino)-1,3-dihydroisobenzofuran-4-carboxylic acid (10): A solution of **9** (0.20 g, 0.83 mmol) in EtOH (15 mL) was treated with K_2CO_3 (0.13 g, 0.94 mmol) and 4-propoxyaniline (0.14 g, 0.93 mmol) and refluxed for 45 min. The solvent was removed in vacuo and the residue partitioned between H_2O and EtOAc. The organic layer was dried over Na_2SO_4 and evaporated in vacuo. Purification of the residue by flash chromatography (EtOAc/MeOH; 9:1) and subsequent recrystallization (acetone/$CHCl_3$) gave **10** as pale-yellow crystals (36 mg, 14%); mp: 206–207 °C; ^{1}H NMR (200 MHz, $CDCl_3$): δ = 1.04 (t, J = 7.4, 3H), 1.72–1.90 (m, 2H), 3.93 (t, J = 6.6, 2H), 5.66 (s, 2H), 6.91 (d, J = 8.8, 2H), 7.53–7.77 (m, 4H), 8.52 (d, J = 7.6, 1H), 18.77 ppm (s, 1H); MS (ESI): m/z 312 $[M+H]^+$.

X-ray crystallography

Single crystals of **3a**,**b** and **10** were submitted for X-ray data collection on a Siemens P4 four-circle diffractometer with graphite monochromated Mo-Kα radiation (λ = 0.71073 Å) at 293 K. The structures were solved by direct methods implemented in SHELXS-97.[24] The refinements were carried out by full-matrix anisotropic least-squares on F2 for all reflections for non-hydrogen atoms using SHELXL-97.[25]

Crystallographic data (excluding structure factors) for the structures of **3a**, **3b**, and **10** have been deposited with the Cambridge Crystallographic Data Centre. CCDC 722320 (**3a**), 722321 (**3b**) and 722322 (**10**) contain the supplementary crystallographic data for this paper. These data can be obtained free of charge from The Cambridge Crystallographic Data Centre via www.ccdc.cam.ac.uk.

Biology

A recombinant fragment of human aggrecan IGD (aggrecan–IGD; Thr331–Gly458) was first digested with aggrecanase. Proteolytic cleavage of the substrate released an aggrecan peptide with the N-terminal sequence AlaArgGlySerValIleLeu (ARGSVIL-peptide), which was then identified by means of two monoclonal antibodies (ELISA module).[22] ARGSVIL-peptide standard curves were run in parallel.

Proteolysis of aggrecan–IGD by aggrecanase: Aggrecan–IGD was incubated with standard recombinant human aggrecanase 1 (ADAMTS-4 amino acids Phe213–Ala579 with a C-terminal tag) or standard recombinant human aggrecanase 2 (ADAMTS-5 amino acids Ser262–Gly625 with a C-terminal tag) in the absence (total enzymatic activity) or presence (modulated enzymatic activity) of the test compounds. Enzymes were pre-incubated with the inhibitors or the appropriate concentration of vehicle as a control (DMSO final concentration of 0.25% in proteolysis), at 4 °C for 30 min prior to assaying their activity. 5 μL of mix enzyme–inhibitor were added to the substrate (final concentration = 0.1 μM) in a total volume of 100 μL and incubated for 15 min at 37 °C. The reaction was terminated with EDTA-containing buffer. The inhibitors were tested at 10 μM final concentration, and compounds achieving > 50% inhibitory effect were evaluated for IC_{50} calculation, in a range generally extended from 0.1 to 10 μM final concentration.

Aggrecan peptide ELISA: ARGSVIL-peptide standard, proteolytic digestion of aggrecan–IGD with standard aggrecanases and test samples were incubated in microtiter wells pre-coated with anti-ARGSVIL-neoepitope antibody. ARGSVIL-peptide was bound to the coated antibody, while other components were removed by washing and aspiration. The bound ARGSVIL-peptide was detected with a second peroxidase-labeled antibody. Any excess of the conjugate was removed by washing and aspiration. The amount of peroxidase bound to different wells was determined by reaction with peroxidase substrate TMB. The reactions were stopped by addition

of sulfuric acid solution and absorbance was read at 450 nm in a microtiter plate spectrophotometer.

Molecular modeling

Inhibitor setup: The structures of the inhibitors used in the docking simulations were generated by means of Discovery Studio software (v 1.5), then minimized using a CHARMm force field.[26] Minimizations were carried out by means of 50 steps of steepest descent and 10000 steps of conjugated gradient as minimization algorithms, with an RMS convergence criterion of 0.01 Å. Partial atomic charges were assigned by means of the Gasteiger–Marsili formalism.[27] All the relevant torsion angles were treated as rotatable during the docking process, thus allowing a search of the conformational space.

Enzymes setup: The ADAMTS-5 protein was set up for docking as follows: polar hydrogens were added by means of Discovery Studio software, and Kollman united-atom partial charges were assigned; ab initio calculated charges were introduced for the prosthetic group.[28] The ADDSOL utility of AutoDock was used to add solvation parameters to the protein structures, and the grid maps representing the proteins in the docking process were calculated using AutoGrid. The grids, one for each atom type in the inhibitor plus one for the electrostatic interactions, were chosen to be large enough to include not only the hypothetical catalytic sites but also a significant part of the protein around it. As a consequence, the dimensions of grid maps were 68 Å × 60 Å × 52 Å with a grid-point spacing of 0.375 Å for ADAMTS-5 for all docking calculations.

Docking calculations: Protonated forms of the inhibitors were docked into the enzymes using AutoDock 4.0. Docking simulations of the compounds were carried out using the Lamarckian genetic algorithm and through a protocol with an initial population of 300 randomly placed individuals, a maximum number of 25 million energy evaluations, a mutation rate of 0.02, a crossover rate of 0.80, and an elitism value of 1. The pseudo-Solis and Wets algorithm with a maximum of 300 interactions was applied for the local search. Two hundred independent docking runs were carried out for each inhibitor, and the resulting conformations that differed by less than 1.0 Å in positional root-mean-square deviation (RMDS) were clustered together. Cluster analysis was performed by selecting the most populated cluster, which in all cases coincided with the one endowed with the best energy.

Acknowledgements

The authors thank Prof. Stefania D'Agata D'Ottavi (Università per Stranieri di Siena, Siena, Italy) for the careful reading of the manuscript, Dr. Roberto Beretta (Rottapharm, Monza, Italy) for combustion analyses, the Consorzio Interuniversitario Nazionale per la Scienza e la Tecnologia dei Materiali (INSTM) for the access to Accelrys software, and Prof. Maria Cristina Menziani (Università di Modena e Reggio Emilia, Modena, Italy) for helpful discussions.

Keywords: ADAMTS · aggrecanase · inhibitors · osteoarthritis · oxoisoindolines · pyrroloquinolinones

[1] J. Martel-Pelletier, *Osteoarthritis Cartilage* **1999**, *7*, 371 – 373.
[2] a) P. J. Roughley, *Eur. Cells Mater.* **2006**, *12*, 92 – 101; b) C. Kiani, L. Chen, Y. J. Wu, A. J. Yee, B. B. Yang, *Cell Res.* **2002**, *12*, 19 – 32; c) T. E. Hardingham, A. J. Fosang, J. Dudhia, *Eur. J. Clin. Chem. Clin. Biochem.* **1994**, *32*, 249 – 257.
[3] a) J. Martel-Pelletier, C. Boileau, J. P. Pelletier, P. J. Roughley, *Best Pract. Res., Clin. Rheumatol.* **2008**, *22*, 351 – 384; b) T. Hardingham, *Curr. Rheumatol. Rep.* **2008**, *10*, 30 – 36; c) R. J. Lories, *Best Pract. Res. Clin. Rheumatol.* **2008**, *22*, 209 – 220; d) M. Hashimoto, T. Nakasa, T. Hikata, H. Asahara, *Med. Res. Rev.* **2008**, *28*, 464 – 481.
[4] a) Y. Rengel, C. Ospelt, S. Gay, *Arthritis Res. Ther.* **2007**, *9*, 221; b) G. S. Firestein, *Curr. Opin. Rheumatol.* **1992**, *4*, 348 – 354; c) M. W. Lark, E. K. Bayne, J. Flanagan, C. F. Harper, L. A. Hoerrner, N. I. Hutchinson, T. T. Singer, S. A. Donatelli, J. R. Weidner, H. R. Williams, R. A. Mumford, L. S. Lohmander, *J. Clin. Invest.* **1997**, *100*, 93 – 106; d) J. D. Sandy, C. Verscharen, *Biochem. J.* **2001**, *358*, 615 – 626.
[5] a) K. D. Brandt, *Am. J. Ther.* **2000**, *7*, 75 – 90; b) H. R. Schumacher, L. X. Chen, *Am. J. Med.* **2005**, *118*, 1208 – 1214; c) A. J. Matheson, C. M. Perry, *Drugs Aging* **2003**, *20*, 1041 – 1060; d) M. Fajardo, P. E. Di Cesare, *Drugs Aging* **2005**, *22*, 141 – 161; e) G. Singh, *Surg. Technol. Int.* **2003**, *11*, 287 – 292; f) J. P. Pelletier, *Osteoarthritis Cartilage* **2004**, *12*, *Suppl. A*, S63 – 68; g) M. C. Hochberg, *Curr. Appl. Phys. Curr. Top Med. Chem.* **2005**, *5*, 443 – 448; h) J. Steinmeyer, Y. T. Konttinen, *Adv. Drug Delivery Rev.* **2006**, *58*, 168 – 211; i) A. J. Fosang, C. B. Little, *Nat. Chem. Biol. Nat. Clin. Rheumatol.* **2008**, *4*, 420 – 427.
[6] a) C. B. Little, C. T. Meeker, S. B. Golub, K. E. Lawlor, P. J. Farmer, S. M. Smith, A. J. Fosang, *J. Clin. Invest.* **2007**, *117*, 1627 – 1636; b) J. D. Sandy, C. R. Flannery, P. J. Neame, L. S. Lohmander, *J. Clin. Invest.* **1992**, *89*, 1512 – 1516.
[7] a) H. Stanton, F. M. Rogerson, C. J. East, S. B. Golub, K. E. Lawlor, C. T. Meeker, C. B. Little, K. Last, P. J. Farmer, I. K. Campbell, A. M. Fourie, A. J. Fosang, *Nature* **2005**, *434*, 648 – 652; b) S. S. Glasson, R. Askew, B. Sheppard, B. Carito, T. Blanchet, H. L. Ma, C. R. Flannery, D. Peluso, K. Kanki, Z. Yang, M. K. Majumdar, E. A. Morris, *Nature* **2005**, *434*, 644 – 648.
[8] A. J. Fosang, F. M. Rogerson, C. J. East, H. Stanton, *Eur. Cells Mater.* **2008**, *15*, 11 – 26.
[9] a) M. C. Noe, V. Natarajan, S. L. Snow, L. A. Wolf-Gouveia, P. G. Mitchell, L. Lopresti-Morrow, L. M. Reeves, S. A. Yocum, I. Otterness, M. A. Bliven, T. J. Carty, J. T. Barberia, F. J. Sweeney, J. L. Liras, M. Vaughn, *Bioorg. Med. Chem. Lett.* **2005**, *15*, 3385 – 3388; b) M. G. Bursavich, A. M. Gilbert, S. Lombardi, K. E. Georgiadis, E. Reifenberg, C. R. Flannery, E. A. Morris, *Bioorg. Med. Chem. Lett.* **2007**, *17*, 1185 – 1188; c) A. M. Gilbert, M. G. Bursavich, S. Lombardi, K. E. Georgiadis, E. Reifenberg, C. R. Flannery, A. E. Morris, *Bioorg. Med. Chem. Lett.* **2007**, *17*, 1189 – 1192; d) M. C. Noe, V. Natarajan, S. L. Snow, P. G. Mitchell, L. Lopresti-Morrow, L. M. Reeves, S. A. Yocum, T. J. Carty, J. A. Barberia, F. J. Sweeney, J. L. Liras, M. Vaughn, J. R. Hardink, J. M. Hawkins, C. Tokar, *Bioorg. Med. Chem. Lett.* **2005**, *15*, 2808 – 2811; e) W. Yao, Z. R. Wasserman, M. Chao, G. Reddy, E. Shi, R.-Q. Liu, M. B. Covington, E. C. Arner, M. A. Pratta, M. Tortorella, R. L. Magolda, R. Newton, M. Qian, M. D. Ribadeneira, D. Christ, R. R. Wexler, C. P. Decicco, *J. Med. Chem.* **2001**, *44*, 3347 – 3350; f) F. De Rienzo, P. Saxena, F. Filomia, G. Caselli, F. Colace, L. Stasi, A. Giordani, M. C. Menziani, *Curr. Med. Chem.* **2009**, *16*, 2395 – 2415.
[10] a) M. Whittaker, C. D. Floyd, P. Brown, A. J. H. Gearing, *Chem. Rev.* **1999**, *99*, 2735 – 2776; b) E. M. Muri, M. J. Nieto, R. D. Sindelar, J. S. Williamson, *Curr. Med. Chem.* **2002**, *9*, 1631 – 1653; c) B. G. Rao, *Curr. Pharm. Des.* **2005**, *11*, 295 – 322.
[11] J. S. Xiang, Y. Hu, T. S. Rush, J. R. Thomason, M. Ipek, P.-E. Sum, L. Abrous, J. J. Sabatini, K. Georgiadis, E. Reifenberg, M. Majumdar, E. A. Morris, S. Tam, *Bioorg. Med. Chem. Lett.* **2006**, *16*, 311 – 316.
[12] a) H.-S. Shieh, K. J. Mathis, J. M. Williams, R. L. Hills, J. F. Wiese, T. E. Benson, J. R. Kiefer, M. H. Marino, J. N. Carroll, J. W. Leone, A.-M. Malfait, E. C. Arner, M. D. Tortorella, A. Tomasselli, *J. Biol. Chem.* **2007**, *283*, 1501 – 1507; b) L. Mosyak, K. Georgiadis, T. Shane, K. Svenson, T. Hebert, T. McDonagh, S. Mackie, S. Olland, L. Lin, X. Zhong, R. Kriz, E. L. Reifenberg, L. A. Collins-Racie, C. Corcoran, B. Freeman, R. Zollner, T. Marvell, M. Vera, P.-E. Sum, E. R. Lavallie, M. Stahl, W. Somers, *Protein Sci.* **2008**, *17*, 16 – 21.
[13] A. Cappelli, M. Anzini, S. Vomero, L. Mennuni, F. Makovec, E. Doucet, M. Hamon, M. C. Menziani, P. G. De Benedetti, G. Giorgi, C. Ghelardini, S. Collina, *Bioorg. Med. Chem.* **2002**, *10*, 779 – 801.
[14] P. B. Hodgson, F. H. Salingue, *Tetrahedron Lett.* **2004**, *45*, 685 – 687.
[15] P. E. Outt, J. J. Ares, G. E. Roberts, X. Wang, T. L. Cupps, F. C. Wireko, *J. Org. Chem.* **1998**, *63*, 5762 – 5768.

[16] S. Mahboobi, A. Sellmer, H. Hocher, C. Garhammer, H. Pongratz, T. Maier, T. Ciossek, T. Beckers, *J. Med. Chem.* **2007**, *50*, 4405 – 4418.
[17] M. Sridhar, B. A. Kumar, R. Narender, *Tetrehedron Lett.* **1998**, *39*, 2847 – 2850.
[18] a) J. E. Francis, K. J. Doebel, P. M. Schutte, E. C. Savarese, S. E. Hopkins, E. F. Bachmann, *Can. J. Chem.* **1979**, *57*, 3320 – 3331; b) C. J. Albisetti, A. L. Barney, T. L. Cairns, H. E. Winberg, (DuPont & Co., Wilmington, Del), US2729622, **1956**; *Chem. Abstr.* 50:60367.
[19] S. J. Grabowski, W. A. Sokalski, E. Dyguda, J. Leszczynski, *J. Phys. Chem. B* **2006**, *110*, 6444 – 6446.
[20] P. Patwari, B. Kurz, J. D. Sandy, A. J. Grodzinsky, *Arch. Biochem. Biophys.* **2000**, *374*, 79 – 85.
[21] P.-E. Sum, D. B. How, J. J. Sabatini, J. S. Xiang, M. Ipek, E. Feyfant, (Wyeth, Madison, NJ), US2007/0043066A1, **2007**; *Chem. Abstr.* 146:163390.
[22] H. Will, M. Dettloff, P. Bendzkô, P. Svenshnikov, *J. Biomol. Tech.* **2005**, *16*, 459 – 472.
[23] G. G. Kleinspehn, J. A. Jung, S. A. Studniarz, *J. Org. Chem.* **1967**, *32*, 460 – 462.
[24] A program for automatic solution of crystal structures, SHELXS-97, developed by G. M. Sheldrick at the University of Göttingen (Göttingen, Germany), **1997**; G. M. Sheldrick, *Acta Crystallogr., Sect. A: Found. Crystallogr.* **2008**, 64, 112 – 122.
[25] G. M. Sheldrick, SHELXL-97, Rel. 97 – 2, A Program for Crystal Structure Refinement, University of Göttingen, Göttingen (Germany), **1997**.
[26] B. R. Brooks, R. E. Bruccoleri, B. D. Olafson, D. J. States, S. Swaminathan, M. Karplus, *J. Comput. Chem.* **1983**, *4*, 187 – 217.
[27] J. Gasteiger, M. Marsili, *Tetrahedron* **1980**, *36*, 3219 – 3228.
[28] A. Khandelwal, V. Lukacova, D. Comez, D. M. Kroll, S. Raha, S. Balaz, *J. Med. Chem.* **2005**, *48*, 5437 – 5447.

Received: December 17, 2009
Revised: March 5, 2010
Published online on April 8, 2010

